

Controllable Traffic Simulation through LLM-Guided Hierarchical Chain-of-Thought Reasoning

Zhiyuan Liu¹, Leheng Li², Yuning Wang¹, Haotian Lin³, Zhizhe Liu⁴, Lei He¹, Jianqiang Wang^{1,†}

Abstract—Evaluating autonomous driving systems in complex and diverse traffic scenarios through controllable simulation is essential to ensure their safety and reliability. However, existing traffic simulation methods face challenges in their controllability. To address this, this paper proposes a novel diffusion-based and LLM-enhanced traffic simulation framework. Our approach incorporates a unique chain-of-thought (CoT) mechanism, which systematically examines the hierarchical structure of traffic elements and guides LLMs to thoroughly analyze traffic scenario descriptions step by step, enhancing their understanding of complex situations. Furthermore, we propose a Frenet-frame-based cost function framework that provides LLMs with geometrically meaningful quantities, improving their grasp of spatial relationships in a scenario and enabling more accurate cost function generation. Experiments on the Waymo Open Motion Dataset (WOMD) demonstrate that our method handles more intricate descriptions, generates a broader range of scenarios in a controllable manner, and outperforms existing diffusion-based methods in terms of efficiency.

I. INTRODUCTION

Autonomous driving has developed rapidly in recent years. To ensure the reliability of these systems, testing on complex, diverse, and long-tailed traffic scenarios through traffic simulation is essential and critical. Early simulation methods, such as rule-based approaches [1]–[3], offered good interpretability but lacked diversity and complexity. In contrast, deep learning techniques [4]–[7] introduced more complexity by learning from large datasets, but they often lack controllability. Without precise control over generated scenarios, it becomes challenging to systematically evaluate how autonomous driving systems respond to specific, critical situations.

To address this problem, recent work has focused on utilizing generative models to achieve controllable traffic simulation. One approach [8]–[10] involves using condition tokens to guide the model with basic conditions, such as goal points or velocity. However, this method requires additional training with the condition tokens and struggles to handle more complex conditions. Another approach leverages conditional sampling in diffusion models, which does not require extra training and offers more flexibility by optimizing cost functions during the sampling process. The cost functions can be either human-designed [11]–[14] or generated by large language models (LLMs) [15]. Human-designed cost functions typically include predefined rules, such as speed

limits or avoiding collisions, but are limited in their ability to address conditions outside of predefined functions. On the other hand, methods based on LLM-generated cost functions mark a significant progression to deal with a wide range of conditions. They take user descriptions of a scenario as input and create corresponding cost functions by LLMs, which is more adaptable than predefined functions. However, current LLMs still face challenges in understanding and processing intricate descriptions. Additionally, due to the complex denoiser architecture and costly sampling process, the diffusion-based approach is notably time-consuming.

Our goal is to overcome the limitations of simulation methods based on diffusion models and LLM-generated cost functions, further utilizing the powerful generative capabilities of LLMs and leveraging the flexibility of diffusion conditional sampling. To achieve this, we first propose a logical framework to guide LLMs in processing complex conditions. Drawing inspiration from research on human behavior, which highlights that humans often break actions down into subtasks [16], we introduce a novel chain-of-thought (CoT) mechanism [17]. This mechanism enables LLMs to systematically break down these events into hierarchical structures, and generate corresponding cost functions step-by-step. By systematically exploring traffic scene elements, we demonstrate the significant advantages of employing CoT to enhance understanding and analysis within this domain.

Furthermore, a proper form of cost functions is needed. Current methods project the trajectories on the surrounding lanes and utilize the projection points to build the cost functions. However, the geometrical implication of the projection is difficult for LLMs to understand, and the process of converting projection points into cost functions is also challenging for them. To address this, we propose a Frenet-frame-based cost function framework, which uses lateral and longitudinal information to build cost functions. The Frenet-based approach has clear geometric meanings and we demonstrate it can further enhance the LLM's understanding of the scenario.

Finally, a more efficient architecture is required. Utilizing the recent techniques in motion prediction [18]–[20], we construct a novel traffic simulation framework. We incorporate the agent's historical trajectories as one of the conditions, eliminating the need for complex historical data encoders. Furthermore, we use a relative coordinate system, thus our method avoids the need to re-encode invariant information like map topology during the rollout of the simulation.

We evaluate our method on the Waymo Open Motion Dataset (WOMD) [21]. Our experiments demonstrate that

¹ School of Vehicle and Mobility, Tsinghua University.

² Artificial Intelligence Thrust, The Hong Kong University of Science and Technology (Guangzhou).

³ School of Computer Science, Carnegie Mellon University.

⁴ Department of Computer Sciences, University of Wisconsin-Madison.

† Corresponding author: wjqlws@tsinghua.edu.cn

the proposed CoT and Frenet-based functions can handle a broader range of conditions compared to existing methods, including typical driving behaviors like cut-ins, as well as abnormal behaviors such as going off-road. Experiments also show that our approach achieves faster generation speeds than the current diffusion-based methods while maintaining competitive performance in the generated scenarios.

Our contributions are summarized as follows:

- We present an innovative CoT mechanism designed to enhance the capability of LLMs to effectively process and interpret the hierarchical structure of elements within traffic simulations, and provide precise guidance for our generative model.
- We develop an efficient diffusion-based traffic simulation framework with faster generation speeds than the current diffusion-based methods while maintaining competitive performance.
- We propose a novel Frenet-frame-based cost function framework that provides clear geometric meanings, making it more understandable and usable by LLMs for building accurate cost functions.
- Thorough experiments show that our method can process more complex descriptions and generate a broader range of scenarios in a controllable manner.

II. RELATED WORK

A. Traffic simulation

Rule-based methods. Early methods utilize heuristic controllers or replayed logs to generate scenarios and use human-designed rules to control the generation [1]–[3]. These methods have good controllability and interpretability. However, they lacked the realism and complexity to capture the full range of real-world situations.

Learning-based methods. Learning-based simulation methods leverage large-scale real-world datasets to simulate driving behaviors [21]–[24]. Early models in this domain [4]–[7] were designed similarly to trajectory prediction models [25], [26] but operated in a closed-loop manner. While these methods provide improved realism, diversity, and complexity, they often lack sufficient controllability. To address this, some approaches incorporate conditional models [8]–[15] to balance both realism and controllability.

Diffusion-based methods. More recent work leverages diffusion models for controllable simulation, benefiting from strong generative capabilities and test-time adaptability. Most of these models [11]–[14], [27] rely on pre-defined functions, such as goal point specification and collision avoidance, to guide the sampling process. While effective, their ability to control conditions beyond these predefined functions is constrained. CTG++ [15] marks a significant progression by utilizing large language models (LLMs) to translate user-specified descriptions into cost functions. This innovation expands the range of controllable conditions, addressing many limitations of previous approaches. However, it still faces challenges in understanding and processing complex descriptions.

B. LLMs for robotics

The application of LLMs in robotics has garnered significant attention due to their ability to bridge the gap between natural language instructions and robotic control. Recent approaches leverage LLMs to generate both actions [28], [29] and reward functions [30], [31], achieving notable progress in this area. Building on these advancements, CTG++ [15] explored the use of LLMs in traffic simulation, employing them to generate cost functions based on natural language descriptions of traffic scenarios. In this work, we aim to extend the generative capabilities of LLMs to construct more comprehensive and precise cost functions, enhancing the controllability of traffic simulations.

III. PRELIMINARY

A. Problem formulation

A traffic scenario can be defined as a combination of road topology M and agent states A . We use a set of N_m polylines for road topology to describe lanes [26], characterized by their coordinates and attributes (such as lane type). In addition, we denote the connectivity of the polylines (predecessor, successor, left neighbor, and right neighbor) as graph edges $E = \{e_{ij}\}$, to represent the road topology. For agent states, we focus primarily on the position and heading of each agent over a sequence of timesteps. An agent's state history and future are denoted as $A_i = \{s_{-T_{\text{hist}}}, \dots, s_0, \dots, s_{T_{\text{future}}}\}$, where $s_t = (x_t, y_t, \theta_t)$. Here, T_{hist} and T_{future} represent the lengths of the history and future trajectories, respectively.

Our goal is to simulate N_a agent future trajectories given (1) the road topology M , (2) the historical states of N_a agents, and (3) the language description specified by the user. These generated trajectories must be consistent with the scenario's language description.

B. Diffusion Models

Diffusion models [32] have emerged as a powerful framework to represent complex data distribution. In general, diffusion models parameterize data distribution as p_θ and learn to model it through score-matching, iteratively transforming a simple distribution such as Gaussian noise into a more complex data distribution through multiple small and reversible steps. The process can be modeled as stochastic differential equations (SDEs) [33] with the forward and reverse process:

$$d\mathbf{x} = f(\mathbf{x}, t)dt + g(t)d\omega \quad (1)$$

$$d\mathbf{x} = [f(\mathbf{x}, t) - g^2(t)\nabla_{\mathbf{x}} \log p_t(\mathbf{x})]dt + g(t)d\omega \quad (2)$$

where ω is the standard Wiener process. $\nabla_{\mathbf{x}} \log p_t(\mathbf{x})$ is the time-dependent score, which can be approximated by training a neural network by score-matching. In our case, diffusion models are used to represent the distribution of trajectory features x conditioned on map topology $p_\theta(x; m)$.

The core of the diffusion process includes designing a series of data distributions that are characterized by noise schedule $\sigma(t)$ and a contraction or scale schedule $s(t)$. In this work, we follow the formulation of EDM [34], which

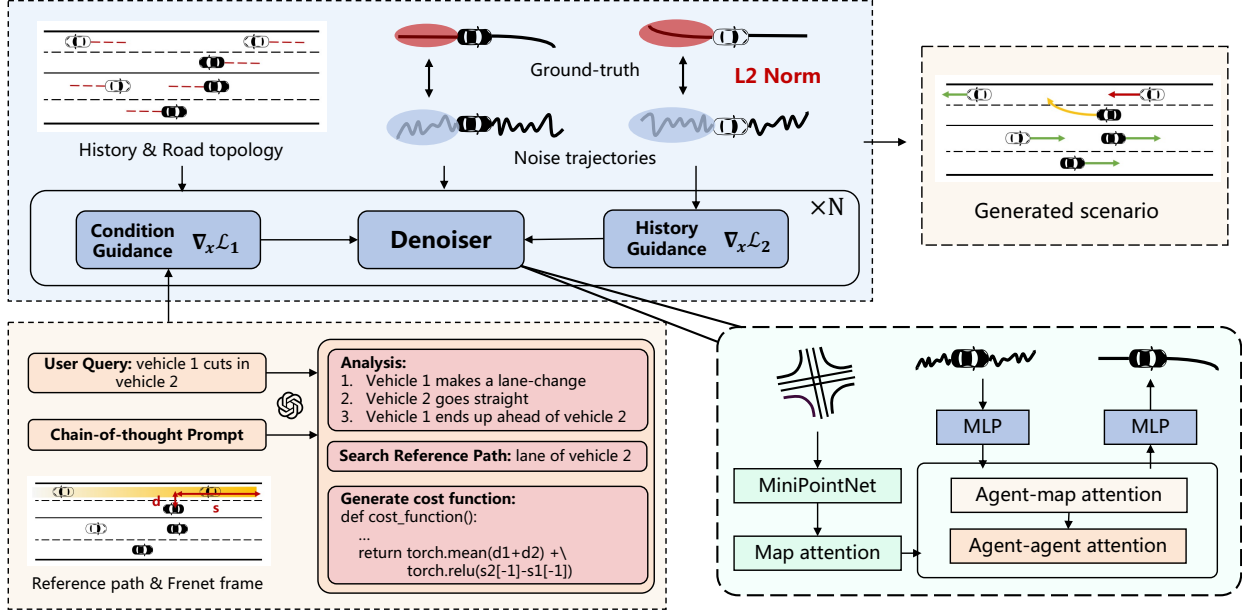


Fig. 1: We propose to leverage the diffusion model to generate future trajectories in a diffusion policy manner. We further carefully design CoT-based prompting to guide the LLM to comprehend and generate the hierarchical structure of traffic scenes. Finally, the guidance generated by LLM is incorporated into the denoiser for controllable generation.

re-designed the diffusion process and depicted the sampling process by the following ODE:

$$d\mathbf{x} = \left[\frac{\dot{s}(t)}{s(t)} \mathbf{x} - s(t)^2 \dot{\sigma}(t) \sigma(t) \nabla_{\mathbf{x}} \log p \left(\frac{\mathbf{x}}{s(t)}; m, \sigma(t) \right) \right] dt \quad (3)$$

In practice, we consider the scaling schedule to be constant $s(t) = 1$. Thus, the ODE in equation (3) simplifies to:

$$d\mathbf{x} = -\dot{\sigma}(t) \sigma(t) \nabla_{\mathbf{x}} \log p(\mathbf{x}; m, \sigma(t)) dt \quad (4)$$

The denoiser model $D_{\theta}(\mathbf{x}; m, \sigma)$ is trained to recover the noised sample \mathbf{x} from its noisy version. The relationship between the score function and the denoiser model is expressed as follows:

$$\nabla_{\mathbf{x}} \log p_{\theta}(\mathbf{x}; m, \sigma) = \frac{D_{\theta}(\mathbf{x}; m, \sigma) - \mathbf{x}}{\sigma^2} \quad (5)$$

During training, the model is optimized by minimizing the following objective:

$$\mathbb{E}_{\mathbf{y} \sim p_0, \mathbf{n} \sim \mathcal{N}(\mathbf{0}, \sigma^2 \mathbf{I})} \|\mathbf{D}_{\theta}(\mathbf{y} + \mathbf{n}; m, \sigma) - \mathbf{y}\|^2, \quad (6)$$

where p_0 is the data distribution and \mathbf{n} represents the Gaussian noise. After training, data can be sampled from noise using the relationship in equation (5) and the ODE described in equation (4).

C. Conditional sampling

For various problems, we have extra condition c which can be described by a cost function \mathcal{L} . In such cases, we aim to sample data from the conditional distribution $p(\mathbf{x}; c)$. Under our specific problem settings, this translates to sampling from $p(\mathbf{x}; m, \sigma, c)$. Consequently, the score function should be modified from $\nabla_{\mathbf{x}} \log p(\mathbf{x}; m, \sigma)$ to $\nabla_{\mathbf{x}} \log p_t(\mathbf{x}; m, \sigma, c)$.

According to Bayes' rule, the modified score function can be expressed as:

$$\nabla_{\mathbf{x}} \log p(\mathbf{x}; c, m, \sigma) = \nabla_{\mathbf{x}} \log p(\mathbf{x}; m, \sigma) + \nabla_{\mathbf{x}} \log p(c; \mathbf{x}, m, \sigma) \quad (7)$$

The first term can be calculated by equation (5), and the second term can be approximated as:

$$\nabla_{\mathbf{x}} \log p(c; \mathbf{x}, m, \sigma) \approx \lambda \frac{\partial}{\partial \mathbf{x}} \mathcal{L}(D_{\theta}(\mathbf{x}; m, \sigma)), \quad (8)$$

where λ is a scaling factor. By utilizing equations (4), (5) and (8), we can sample data that meets the condition c . In practice, to ensure the stability of the sampling process, a score threshold of $(-1, 1)$ is applied to equation (8).

IV. METHOD

The overall framework of our proposed method is illustrated in Figure 1. In this section, we first introduce the **Transformer-based Denoiser**, which models the complex interactions within traffic scenarios (see Section IV-A). Following this, we detail the **Guided Generation** module. As providing clear guidance for denoiser is non-trivial, we introduce the chain-of-thought mechanism and Frenet-based cost functions (see Section IV-B) to generate the hierarchical structure of traffic scenes.

A. Transformer-based denoiser

Relative coordinate system. In alignment with recent trajectory prediction methods [18], [19], we adopt a relative coordinate system. Initially, road polylines and trajectories are rotated and normalized to the central or current position. To further capture spatial relationships among traffic elements, the feature vector $\mathbf{d}_{ij} = (\Delta x_{ij}, \Delta y_{ij}, \cos \Delta \theta_{ij}, \sin \Delta \theta_{ij})$ is extracted, where $(\Delta x_{ij}, \Delta y_{ij})$ represents the relative positions within the reference frame of agent i , and $\Delta \theta_{ij}$ denotes the

relative heading angle. Note that the feature vectors between static elements, such as road polylines, remain consistent regardless of the agents' movements. Consequently, this approach eliminates the need to re-encode the map topology during simulation rollout, thereby enhancing inference speed.

Latent trajectory expression. Following recent studies [12], we use Principal Component Analysis (PCA) to express trajectories in the latent space. Specifically, for each trajectory $A_i \in \mathbb{R}^{T \times 3}$, PCA maps it into the latent representation $\tilde{A}_i \in \mathbb{R}^{d_{PCA}}$, where d_{PCA} is the number of principal components. The latent expression captures both spatial and temporal features, enabling the model to encode trajectories directly with a Multi-Layer Perceptron (MLP) at a low computational cost, rather than employing models like attention mechanisms with high computational overhead.

History guidance. Current methods [12], [15] utilize complex encoders to model historical information, directly learning the distribution $p(x; m, A_{\text{hist}})$. Our approach, however, treats the historical states A_{hist} as an additional condition rather than embedding it directly into the model. Consequently, our model learns the distribution $p(x; m)$ and employs the sampling method introduced in Section III-C to generate data conditioned on historical states. Specifically, we express this condition using the L2 norm between the generated trajectory history \mathbf{y}_{hist} and the ground-truth history $\hat{\mathbf{y}}_{\text{hist}}$:

$$\mathcal{L}_{\text{hist}} = \|\mathbf{y}_{\text{hist}} - \hat{\mathbf{y}}_{\text{hist}}\|^2 \quad (9)$$

By incorporating this additional loss term within the framework of controllable simulation, we effectively integrate historical information without the need for a separate encoder, simplifying the overall model design and enhancing computational efficiency.

Model architecture. The model architecture is shown in the bottom right of Figure 1. We employ a MiniPointNet [35] which is primarily composed of max pooling and MLPs to obtain polyline-level features from the road topology feature M . The encoding process can be expressed as:

$$X_m = \text{MiniPointNet}(M), X_m \in \mathbb{R}^{N_m \times d} \quad (10)$$

where X_m is the polyline-level feature and d denotes the hidden size of the model. For agent features $X_a \in \mathbb{R}^{N_a \times d}$, we utilize an MLP to encode the noise trajectories in the PCA latent space.

After feature encoding, we employ three distinct attention modules to extract the lane-lane, agent-lane, and agent-agent interactions. Let \mathbf{x}_i denote the feature of an object, the attention mechanism can be expressed as:

$$\tilde{\mathbf{x}}_i = \sum_j \text{Softmax}(s_{ij})(\mathbf{x}_j \mathbf{W}_v + \text{MLP}(\mathbf{r}_{ij})), \quad (11)$$

$$s_{ij} = \frac{1}{\sqrt{d}}(\mathbf{x}_i \mathbf{W}_q)(\mathbf{x}_j \mathbf{W}_k + \text{MLP}(\mathbf{r}_{ij})), \quad (12)$$

where \mathbf{W} represents a Linear layer. For agent-agent and agent-lane attentions, \mathbf{r}_{ij} is the spatial relativity feature \mathbf{d}_{ij} . For lane-lane attentions, $\mathbf{r}_{ij} = \mathbf{d}_{ij} + \mathbf{e}_{ij}$ is the sum of the spatial relativity feature and the connectivity feature.

B. Guided generation

Chain-of-thought mechanism. Our goal is to convert user descriptions into cost functions using LLMs and guide the generation through the method outlined in III-C. Existing methods often struggle with processing and understanding complex descriptions. Our approach leverages a chain-of-thought (CoT) mechanism to systematically break down these events into hierarchical structures, and generate corresponding cost functions step-by-step, ensuring accurate interpretation and alignment of traffic participant trajectories.

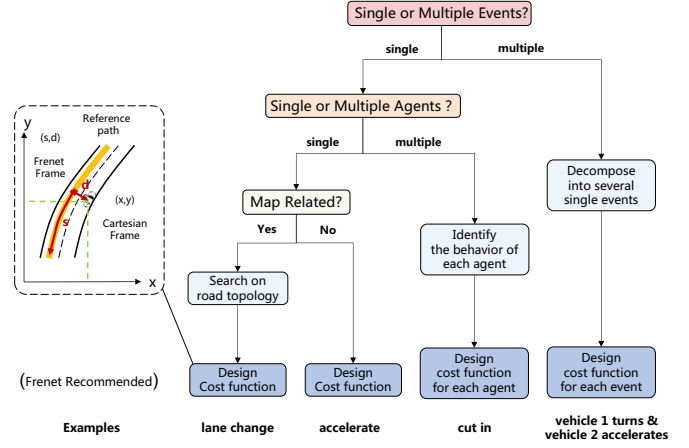


Fig. 2: Utilizing a logic relation diagram and examining the hierarchical structure of traffic elements, we employ the chain-of-thought mechanism to thoroughly analyze and interpret these hierarchical behaviors for controllable generation.

Figure 2 illustrates the detailed CoT process. First, recognize the events. For multiple events, break them down into several single events. Then, determine the number of agents involved. If multiple agents are involved, identify each agent's behavior. Next, assess whether each behavior is map-related. If it is, design an algorithm to explore the road topology $E = \{e_{ij}\}$. Finally, generate cost functions. For map-related descriptions, Frenet-based cost functions are recommended. We will show that with this step-by-step thinking manner, the LLM can effectively understand and process a wider range of complex descriptions.

Frenet-based cost functions. Inspired by the success of the Frenet frame in motion planning, we utilize it to construct cost functions for descriptions related to map information. The Frenet frame is shown on the left side of Figure 2. It describes the relative position of trajectories concerning the reference path by the longitudinal distance s and the lateral offset d , which have clear geometric meanings, making them easy for LLMs to understand and utilize. LLMs will generate cost functions based on s and d , enabling the control of both longitudinal and lateral directions. We will demonstrate that using these Frenet-based cost functions significantly enhances the LLMs' understanding of spatial relationships within traffic scenarios, leading to a substantial improvement in their ability to generate accurate cost functions.

Category	Method	ADE (m) ↓	FDE (m) ↓	JSD ($\times 10^{-2}$) ↓	Collision (%) ↓	Off Road (%) ↓	Per Scene Gen. Time (s) ↓
Auto-regressive Methods	Actions-Only [36]	4.81	11.89	10.4	19.9	27.6	3.3
	Decision Transformer [37]	1.56	3.07	8.4	5.3	11.0	20.7
	CtRL-Sim [9]	1.25	2.04	<u>7.9</u>	5.3	11.0	8.2
Diffusion-based Methods	CTG++ [15]	1.73	4.02	7.4	5.9	15.0	44.0
	Ours (32 diffusion steps)	1.17	1.93	8.2	<u>5.1</u>	<u>12.8</u>	20.4
	Ours (50 diffusion steps)	<u>1.18</u>	<u>1.97</u>	8.6	4.9	13.2	29.1

TABLE I: Results of traffic simulation on WOMD. We **bolded** the optimal result and underlined the second best result.

V. EXPERIMENTS

A. Experiment Setup

Dataset. Our experiments are conducted on large-scale real-world traffic scenario dataset: the Waymo Open Motion Dataset (WOMD) [21]. WOMD comprises over 570 hours of 10hz scenario data. We train our model on the entire training split, which contains 69,500 scenarios and evaluate it on a subset of 1,000 scenarios from validation split.

Evaluation. We begin by conducting traffic simulation experiments, following the experimental settings of CtRL-Sim [9]. Using a 1.1-second history and road topology as input, we simulate the future trajectories over an 8-second horizon. We use the Final Displacement Error (**FDE**) and Average Displacement Error (**ADE**) to measure reconstruction error. We employ a distributional metric (**JSD**) to evaluate realism, defined as the mean of the Jensen-Shannon Distances computed on linear speed, angular speed, acceleration, and distance to the nearest vehicle between real and simulated scenes. Additionally, common-sense metrics like **Collision** rate and **Offroad** rate are used.

Given our flexible model design, which does not require encoding historical data, our model can handle input consisting solely of a single frame of agent state and road topology, which is consistent with the problem setting for scenario generation. Thus, we further perform experiments on traffic scenario generation to validate the model. In line with experimental settings in this area, we evaluate the model using scene collision rate (**SCR**) and the Maximum Mean Discrepancy (**MMD**) metrics for both distance to the nearest object features (MMD_o) and distance to road edge features (MMD_r).

Lastly, we conduct experiments on controllable scenario generation. We select a range of common or complex scenario descriptions, and evaluate whether the generated cost functions accurately reflect these descriptions. We also visualize the results to assess if the model correctly follows the guidance of the generated functions for each scenario.

Baselines. For traffic simulation, we compare our method against recent auto-regressive methods, including Actions-Only (a modified version of Trajeglish [36]), Decision Transformer [37], and CtRL-Sim [9]. We also include the popular diffusion-based method CTG++ [15]. For scenario generation, we compare our approach to TrafficGen [38] and LCTGen [39]. In the controllable generation experiments, we compare the expressiveness of our CoT mechanism combined

with Frenet-frame-based cost functions against the CTG++ prompt method.

Implementation Details. We set the number of layers for all attention modules to 3. The number of agents is set to $N_a = 24$, and the number of lane polylines to $N_m = 200$. We use 32 sampling steps for diffusion sampling, with other hyperparameters following EDM [34]. For closed-loop simulation, we set the re-plan rate to 2 Hz. For controllable generation, we use GPT4 [40] for cost function generation.

B. Traffic simulation results

The traffic simulation results are presented in Table I. In alignment with the experimental setup, we query the LLM with the instruction "vehicle should reach *target_point* and avoid collisions," and then the generated cost function is used to guide the model. Our model achieves the best reconstruction performance and ranks second in terms of common-sense metrics. However, the JSD metric is slightly inferior to the current state-of-the-art methods. A potential reason for this is that our method directly outputs future states, whereas other methods generate actions, which may lead to better dynamic feasibility. As for generation speed, our model demonstrates a significant advantage over diffusion-based CTG++ and is competitive to some auto-regressive methods.

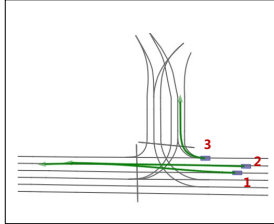
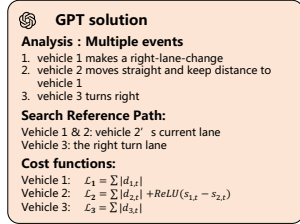
Method	Per Scene Generation Time (s)	
	w/o map reuse	w map reuse
CTG++	44.0	-
Ours (50 diffusion steps)	32.5	29.1
Ours (32 diffusion steps)	23.2	20.4

TABLE II: Comparison of generation time with CTG++.

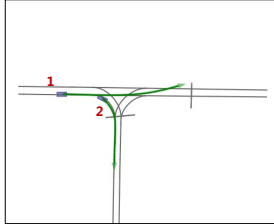
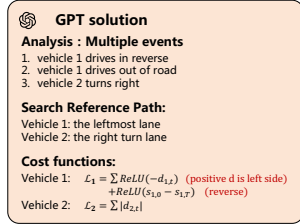
Method	SCR(%) ↓	MMD_o ↓	MMD_r ↓
TrafficGen [38]	9.7	0.31	0.23
LCTGen [39]	11.2	0.27	0.33
Ours	6.3	0.24	0.17

TABLE III: Results of traffic scenario generation.

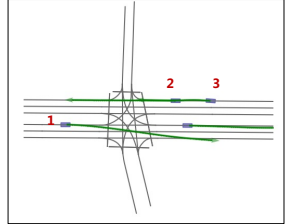
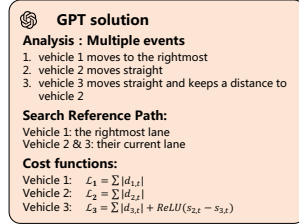
To further validate the efficiency of our design, we conduct an ablation experiment presented in Table II. In addition to our 32-diffusion-step version, we also evaluate our method using 50 diffusion steps to align with CTG++. By incorporating historical data through conditional sampling, our model eliminates the need for historical data encoders, resulting



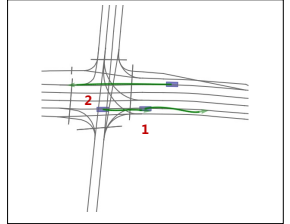
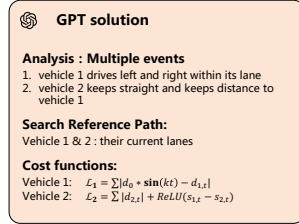
(a) User query: vehicle 1 cuts in vehicle 2, while vehicle 3 turns right.



(c) User query: vehicle 1 drives in reverse and out of the road, while vehicle 2 turns right.



(b) User query: vehicle 1 moves to the rightmost, while vehicle 2 drives straight and vehicle 3 follows vehicle 2.



(d) User query: vehicle 1 drives left and right within its lane, and vehicle 2 keeps straight and follows vehicle 1.

Fig. 3: GPT solutions and visualizations for some cases.

in a considerable speedup. Moreover, by leveraging relative coordinates to enable map reuse, the generation speed is further enhanced.

The results of traffic generation are shown in Table III. Our model outperforms others across all metrics, further confirming its ability to generate realistic traffic scenarios.

C. Controllable simulation results

We test a range of descriptions including basic rules, complex interactions and abnormal behaviors as shown in Table IV. To assess the contribution of each component, we conduct an ablation study.

In terms of basic rules, all tested methods demonstrated effective performance by employing functions like Norm for target point and ReLU for speed limit. These results suggest that LLMs do not confine the generation of cost functions to recommended forms (e.g., projection or Frenet), but instead allow for diverse, adaptable cost function formulations.

When addressing interactions such as lane changes, all methods performed well. However, for more complex road topologies—such as navigating the rightmost lane and approaching the next intersection—CoT methods demonstrated superior performance due to their enhanced map exploration capabilities. In agent interactions like cut-ins, CoT effectively understands and processes them by recognizing that one vehicle continues straight while another performs a lane change into its path, while CTG++ struggles to understand them. Although CoT correctly understands these behaviors, projection-based methods still occasionally generate incorrect cost functions. In contrast, the Frenet-based approach consistently performs accurately, as its clear geometric interpretations further enhance the LLM’s understanding of the scenario.

Regarding abnormal behaviors, the CoT+Frenet approach demonstrates impressive performance. The LLM generates

$\sin(d)$ to simulate the vehicle swaying left and right within the lane, and controls d to be positive, ensuring the vehicle stays on the left side of the road edge. The Frenet-based approach allows the LLM to express these abnormal behaviors with concise function forms, highlighting the expressiveness of the Frenet frame and its ability to enhance the LLM’s understanding of complex traffic scenarios. Additionally, this capability to generate abnormal behaviors is particularly valuable for simulating long-tail scenarios.

Category	Description	CTG++	CoT+ Projection	CoT+ Frenet
Basic rules	vehicle drives at a speed limit 10m/s vehicle reaches target point (25, 25) no collisions between all vehicles	✓ ✓ ✓	✓ ✓ ✓	✓ ✓ ✓
Complex interactions	vehicle makes a left-lane-change vehicle moves to the rightmost lane vehicle turns right at the next intersection vehicle 1 cuts in vehicle 2	✓ ✓ ✓ ✓	✓ ✓ ✓ ✓	✓ ✓ ✓ ✓
Abnormal behaviors	vehicle drives in reverse vehicle drives out of the road vehicle drives left and right within the lane	✓ ✓ ✓	✓ ✓ ✓	✓ ✓ ✓

TABLE IV: Results of controllable simulation.

We further combine some descriptions then query the LLM, and visualize the generation results, as shown in Fig 3. The LLM effectively decomposed the complex descriptions and generated the correct forms of cost functions. The visualizations further demonstrate that the model accurately follows the guidance of the generated functions.

VI. CONCLUSION

In this paper, we proposed a novel CoT-enhanced traffic simulation model. Our framework is constructed on a diffusion-based generative model, which we have optimized for enhanced computational efficiency and controllability. Our method is capable of taking users’ descriptions as input, and generate a wide range of scenarios, including complex interactions and long-tail events. We hope our method will offer significant contributions to the field.

REFERENCES

[1] P. A. Lopez, M. Behrisch, L. Bieker-Walz, J. Erdmann, Y.-P. Flötteröd, R. Hilbrich, L. Lücke, J. Rummel, P. Wagner, and E. Wiessner, "Microscopic traffic simulation using sumo," in *2018 21st International Conference on Intelligent Transportation Systems (ITSC)*, 2018, pp. 2575–2582.

[2] M. Treiber, A. Hennecke, and D. Helbing, "Congested traffic states in empirical observations and microscopic simulations," *Physical Review E*, vol. 62, no. 2, p. 1805–1824, Aug. 2000. [Online]. Available: <http://dx.doi.org/10.1103/PhysRevE.62.1805>

[3] G. Rong, B. H. Shin, H. Tabatabaei, Q. Lu, S. Lemke, M. Možeiko, E. Boise, G. Uhm, M. Gerow, S. Mehta, *et al.*, "Lgsvl simulator: A high fidelity simulator for autonomous driving," *arXiv preprint arXiv:2005.03778*, 2020.

[4] S. Suo, S. Regaldo, S. Casas, and R. Urtasun, "Trafficsim: Learning to simulate realistic multi-agent behaviors," in *Proceedings of the IEEE/CVF Conference on Computer Vision and Pattern Recognition*, 2021, pp. 10400–10409.

[5] D. Xu, Y. Chen, B. Ivanovic, and M. Pavone, "Bits: Bi-level imitation for traffic simulation," in *2023 IEEE International Conference on Robotics and Automation (ICRA)*, 2023, pp. 2929–2936.

[6] L. Bergamini, Y. Ye, O. Scheel, L. Chen, C. Hu, L. Del Pero, B. Osiński, H. Grismett, and P. Ondruska, "Simnet: Learning reactive self-driving simulations from real-world observations," in *2021 IEEE International Conference on Robotics and Automation (ICRA)*, 2021, pp. 5119–5125.

[7] A. Kamenev, L. Wang, O. B. Bohan, I. Kulkarni, B. Kartal, A. Molchanov, S. Birchfield, D. Nistér, and N. Smolyanskiy, "Predictionnet: Real-time joint probabilistic traffic prediction for planning, control, and simulation," in *2022 International Conference on Robotics and Automation (ICRA)*. IEEE, 2022, pp. 8936–8942.

[8] E. Pronovost, M. R. Ganesina, N. Hendy, Z. Wang, A. Morales, K. Wang, and N. Roy, "Scenario diffusion: Controllable driving scenario generation with diffusion," *Advances in Neural Information Processing Systems*, vol. 36, pp. 68 873–68 894, 2023.

[9] L. Rowe, R. Giris, A. Gosselin, B. Carrez, F. Golemo, F. Heide, L. Paull, and C. Pal, "Ctrl-sim: Reactive and controllable driving agents with offline reinforcement learning," 2024. [Online]. Available: <https://arxiv.org/abs/2403.19918>

[10] S. Wang, G. Sun, F. Ma, T. Hu, Y. Song, L. Zhu, and M. Liu, "Dragtraffic: A non-expert interactive and point-based controllable traffic scene generation framework," 2024. [Online]. Available: <https://arxiv.org/abs/2404.12624>

[11] Z. Zhong, D. Rempe, D. Xu, Y. Chen, S. Veer, T. Che, B. Ray, and M. Pavone, "Guided conditional diffusion for controllable traffic simulation," in *2023 IEEE International Conference on Robotics and Automation (ICRA)*. IEEE, 2023, pp. 3560–3566.

[12] C. Jiang, A. Cornman, C. Park, B. Sapp, Y. Zhou, D. Anguelov, *et al.*, "Motondiffuser: Controllable multi-agent motion prediction using diffusion," in *Proceedings of the IEEE/CVF Conference on Computer Vision and Pattern Recognition*, 2023, pp. 9644–9653.

[13] W.-J. Chang, F. Pittaluga, M. Tomizuka, W. Zhan, and M. Chandraker, "Controllable safety-critical closed-loop traffic simulation via guided diffusion," *arXiv preprint arXiv:2401.00391*, 2023.

[14] C. Xu, D. Zhao, A. Sangiovanni-Vincentelli, and B. Li, "Diffscene: Diffusion-based safety-critical scenario generation for autonomous vehicles," in *The Second Workshop on New Frontiers in Adversarial Machine Learning*, 2023. [Online]. Available: <https://openreview.net/forum?id=hclEbdHida>

[15] Z. Zhong, D. Rempe, Y. Chen, B. Ivanovic, Y. Cao, D. Xu, M. Pavone, and B. Ray, "Language-guided traffic simulation via scene-level diffusion," in *Conference on Robot Learning*. PMLR, 2023, pp. 144–177.

[16] A. Solway, C. Diuk, N. C  rdova, D. Yee, A. G. Barto, Y. Niv, and M. M. Botvinick, "Optimal behavioral hierarchy," *PLoS computational biology*, vol. 10, no. 8, p. e1003779, 2014.

[17] J. Wei, X. Wang, D. Schuurmans, M. Bosma, B. Ichter, F. Xia, E. Chi, Q. Le, and D. Zhou, "Chain-of-thought prompting elicits reasoning in large language models," 2023. [Online]. Available: <https://arxiv.org/abs/2201.11903>

[18] Z. Zhou, J. Wang, Y.-H. Li, and Y.-K. Huang, "Query-centric trajectory prediction," in *Proceedings of the IEEE/CVF Conference on Computer Vision and Pattern Recognition*, 2023, pp. 17 863–17 873.

[19] S. Shi, L. Jiang, D. Dai, and B. Schiele, "Mtr++: Multi-agent motion prediction with symmetric scene modeling and guided intention querying," *arXiv preprint arXiv:2306.17770*, 2023.

[20] H. Lin, Y. Wang, M. Huo, C. Peng, Z. Liu, and M. Tomizuka, "Joint pedestrian trajectory prediction through posterior sampling," *arXiv preprint arXiv:2404.00237*, 2024.

[21] S. Ettinger, S. Cheng, B. Caine, C. Liu, H. Zhao, S. Pradhan, Y. Chai, B. Sapp, C. R. Qi, Y. Zhou, Z. Yang, A. Chouard, P. Sun, J. Ngiam, V. Vasudevan, A. McCauley, J. Shlens, and D. Anguelov, "Large scale interactive motion forecasting for autonomous driving: The waymo open motion dataset," in *Proceedings of the IEEE/CVF International Conference on Computer Vision (ICCV)*, October 2021, pp. 9710–9719.

[22] M.-F. Chang, J. Lambert, P. Sangkloy, J. Singh, S. Bak, A. Hartnett, D. Wang, P. Carr, S. Lucey, D. Ramanan, *et al.*, "Argoverse: 3d tracking and forecasting with rich maps," in *Proceedings of the IEEE/CVF conference on computer vision and pattern recognition*, 2019, pp. 8748–8757.

[23] B. Wilson, W. Qi, T. Agarwal, J. Lambert, J. Singh, S. Khandelwal, B. Pan, R. Kumar, A. Hartnett, J. K. Pontes, *et al.*, "Argoverse 2: Next generation datasets for self-driving perception and forecasting," *arXiv preprint arXiv:2301.00493*, 2023.

[24] H. Caesar, V. Bankiti, A. H. Lang, S. Vora, V. E. Liong, Q. Xu, A. Krishnan, Y. Pan, G. Baldan, and O. Beijbom, "nuscenes: A multimodal dataset for autonomous driving," *arXiv preprint arXiv:1903.11027*, 2019.

[25] B. Varadarajan, A. Hefny, A. Srivastava, K. S. Refaat, N. Nayakanti, A. Cornman, K. Chen, B. Douillard, C. P. Lam, D. Anguelov, *et al.*, "Multipath++: Efficient information fusion and trajectory aggregation for behavior prediction," in *2022 International Conference on Robotics and Automation (ICRA)*. IEEE, 2022, pp. 7814–7821.

[26] J. Gao, C. Sun, H. Zhao, Y. Shen, D. Anguelov, C. Li, and C. Schmid, "Vectornet: Encoding hd maps and agent dynamics from vectorized representation," in *Proceedings of the IEEE/CVF Conference on Computer Vision and Pattern Recognition*, 2020, pp. 11 525–11 533.

[27] Z. Huang, Z. Zhang, A. Vaidya, Y. Chen, C. Lv, and J. F. Fisac, "Versatile scene-consistent traffic scenario generation as optimization with diffusion," 2024.

[28] O. Mees, J. Borja-Diaz, and W. Burgard, "Grounding language with visual affordances over unstructured data," in *2023 IEEE International Conference on Robotics and Automation (ICRA)*, 2023, pp. 11 576–11 582.

[29] C. Lynch, A. Wahid, J. Tompson, T. Ding, J. Betker, R. Baruch, T. Armstrong, and P. Florence, "Interactive language: Talking to robots in real time," *IEEE Robotics and Automation Letters*, pp. 1–8, 2023.

[30] J. Lin, D. Fried, D. Klein, and A. Dragan, "Inferring rewards from language in context," in *Proceedings of the 60th Annual Meeting of the Association for Computational Linguistics (Volume 1: Long Papers)*. Dublin, Ireland: Association for Computational Linguistics, May 2022, pp. 8546–8560. [Online]. Available: <https://aclanthology.org/2022.acl-long.585>

[31] W. Yu, N. Gileadi, C. Fu, S. Kirmani, K.-H. Lee, M. Gonzalez Arenas, H.-T. Lewis Chiang, T. Erez, L. Hasenklever, J. Humprik, B. Ichter, T. Xiao, P. Xu, A. Zeng, T. Zhang, N. Heess, D. Sadigh, J. Tan, Y. Tassa, and F. Xia, "Language to rewards for robotic skill synthesis," *Conference of Robot Learning 2023*, 2023.

[32] J. Ho, A. Jain, and P. Abbeel, "Denoising diffusion probabilistic models," *Advances in neural information processing systems*, vol. 33, pp. 6840–6851, 2020.

[33] Y. Song, J. Sohl-Dickstein, D. P. Kingma, A. Kumar, S. Ermon, and B. Poole, "Score-based generative modeling through stochastic differential equations," *arXiv preprint arXiv:2011.13456*, 2020.

[34] T. Karras, M. Aittala, T. Aila, and S. Laine, "Elucidating the design space of diffusion-based generative models," *Advances in Neural Information Processing Systems*, vol. 35, pp. 26 565–26 577, 2022.

[35] C. R. Qi, H. Su, K. Mo, and L. J. Guibas, "Pointnet: Deep learning on point sets for 3d classification and segmentation," 2017.

[36] J. Philion, X. B. Peng, and S. Fidler, "Trajeglish: Traffic modeling as next-token prediction," in *The Twelfth International Conference on Learning Representations*, 2024. [Online]. Available: <https://openreview.net/forum?id=Z59Rb5bPPP>

[37] L. Chen, K. Lu, A. Rajeswaran, K. Lee, A. Grover, M. Laskin, P. Abbeel, A. Srinivas, and I. Mordatch, "Decision transformer: Reinforcement learning via sequence modeling," in *Advances in Neural Information Processing Systems*, M. Ranzato, A. Beygelzimer, Y. Dauphin, P. Liang, and J. W. Vaughan, Eds., vol. 34. Curran Associates, Inc., 2021, pp. 15 084–15 097. [Online]. Available: https://proceedings.neurips.cc/paper_files/paper/2021/file/7f489f642a0ddb10272b5c31057f0663-Paper.pdf

- [38] L. Feng, Q. Li, Z. Peng, S. Tan, and B. Zhou, “Trafficgen: Learning to generate diverse and realistic traffic scenarios,” in *2023 IEEE International Conference on Robotics and Automation (ICRA)*. IEEE, 2023, pp. 3567–3575.
- [39] S. Tan, B. Ivanovic, X. Weng, M. Pavone, and P. Krahenbuehl, “Language conditioned traffic generation,” in *7th Annual Conference on Robot Learning*, 2023. [Online]. Available: <https://openreview.net/forum?id=PK2debCKaG>
- [40] J. Achiam, S. Adler, S. Agarwal, L. Ahmad, I. Akkaya, F. L. Aleman, D. Almeida, J. Altenschmidt, S. Altman, S. Anadkat, *et al.*, “Gpt-4 technical report,” *arXiv preprint arXiv:2303.08774*, 2023.